Momentum Spectroscopy of 1D Phase Fluctuations in Bose-Einstein Condensates

S. Richard, F. Gerbier, J. H. Thywissen,* M. Hugbart, P. Bouyer, and A. Aspect
Laboratoire Charles Fabry de l'Institut d'Optique, UMR 8501 du CNRS, 91403 Orsay Cedex, France
(Received 7 March 2003; published 3 July 2003)

We measure the axial momentum distribution of Bose-Einstein condensates with an aspect ratio of 152 using Bragg spectroscopy. We observe the Lorentzian momentum distribution characteristic of one-dimensional phase fluctuations. The temperature dependence of the width of this distribution provides a quantitative test of quasicondensate theory. In addition, we observe a condensate length consistent with the suppression of density fluctuations, even when phase fluctuations are large.

DOI: 10.1103/PhysRevLett.91.010405 PACS numbers: 03.75.Hh, 03.75.Nt, 05.30.Jp

One of the most striking features of Bose-Einstein condensates is their phase coherence. Extensive experimental work on dilute atomic gases has demonstrated a uniform phase of three-dimensional (3D) trapped condensates [1,2], even at finite temperature [3]. In low dimensional systems, however, phase fluctuations of the order parameter are expected to destroy off-diagonal long range order (see [4,5] and references therein). This phenomenon also occurs in sufficiently anisotropic 3D samples, where phase coherence across the axis (long dimension) is established only below a temperature T_ϕ, that can be much lower than the critical temperature T_c [6]. In the range $T_\phi < T < T_c$, the cloud is a "quasicondensate," whose incomplete phase coherence is due to thermal excitations of 1D axial modes, with wavelengths larger than its radial size. Quasicondensates in elongated traps have been observed by Dettmer *et al.* [7], who measured the conversion, during free expansion, of the phase fluctuations into ripples in the density profile. Although the conversion dynamics is well understood [8], the measured amplitude of density ripples was a factor of 2 smaller than expected. In addition, nonequilibrium phase fluctuations in elongated condensates have been observed with the condensate focusing method [9].

In this Letter, we report on the measurement of the axial coherence properties of quasicondensates via momentum Bragg spectroscopy. In previous work using this technique [2,10], the finite size and mean-field energy were the primary contributors to the spectral width. By contrast, the dominant broadening in our conditions results from thermally driven fluctuations of the phase, which reduce the coherence length [4,6]. Indeed, the axial momentum distribution is the Fourier transform of the spatial correlation function $C(s) = \int d^3\mathbf{r}\,\langle\hat{\Psi}^\dagger(\mathbf{r} - s\mathbf{u}_z/2)\hat{\Psi}(\mathbf{r} + s\mathbf{u}_z/2)\rangle$ [11], where $\mathbf{u}_z$ is the axial unit vector. When phase fluctuations dominate (i.e., $T \gg T_\phi$), the axial momentum width is, hence, proportional to $\hbar/L_\phi$, where L_ϕ is the characteristic axial decay length of $C(s)$. Experimentally, for $6 < T/T_\phi < 28$, we find momentum distributions with Lorentzian shapes, whose widths increase with T. Such a shape is characteristic of large phase fluctuations in 1D [12], which result in a nearly exponential decay of $C(s)$. Moreover, the momentum half-width Δp agrees quantitatively with theoretical predictions to within our 15% experimental uncertainty. This implies, in this temperature range, a coherence length $\hbar/\Delta p$ substantially smaller than the quasicondensate length $2L$, from about $L/18$ to $L/4$ [13]. We have also checked an important feature of quasicondensates: the suppression of density fluctuations even in the presence of large phase fluctuations.

We produce a Bose-Einstein condensate of ^{87}Rb in the $5S_{1/2}\,|F = 1, m_F = -1\rangle$ state. A new design of our iron-core electromagnet, with respect to our previous work [14], allows us to lower the bias field of the Ioffe-Pritchard trap to obtain tighter radial confinement. Final radial and axial trap frequencies are, respectively, $\omega_\perp/2\pi = 760(20)$ and $\omega_z/2\pi = 5.00(5)$ Hz. The condensates, containing around 5×10^4 atoms [15], are needle shaped, with a typical half-length $L \simeq 130$ μm and radius $R \simeq 0.8$ μm. The chemical potential being a few times $\hbar\omega_\perp$, the clouds are between the 3D and 1D Thomas-Fermi regime [17]. However, the low-lying excitations of the condensate are 1D in character, due to the large aspect ratio of the trap [18].

Our momentum distribution measurement is based on four-photon velocity-selective Bragg diffraction [2,10,11,19]. Atoms are diffracted out of the condensate by a moving standing wave, formed by two counterpropagating laser beams with a relative detuning δ. Because of the Doppler effect, the momentum component resonantly diffracted out of the condensate is $p_z = M(\delta - 8\omega_R)/(2k_L)$ with $\omega_R = \hbar k_L^2/(2M)$, M the atomic mass, and $k_L = 2\pi/\lambda$ ($\lambda = 780.02$ nm). The lasers are tuned 6.6 GHz below resonance to avoid Rayleigh scattering. The laser intensities (about 2 mW/cm^2) are adjusted to keep the diffraction efficiency below 20%.

To build the momentum spectrum of the quasicondensate, we measure the fraction of diffracted atoms versus the detuning δ between the Bragg laser beams. The differential frequency δ must be stable to better than the desired spectral resolution, about 200 Hz for our typical $L_\phi = 10$ μm. The optical setup is as follows. A single laser beam is spatially filtered by a fiber optic,

separated into two arms with orthogonal polarizations, frequency shifted by two independent 80 MHz acousto-optic modulators, and recombined. The modulators are driven by two synthesizers stable to better than 1 Hz over the typical acquisition time of a spectrum. The overlapping, recombined beams are then sent through the vacuum cell, parallel (to within 1 mrad) to the long axis of the trap, and retroreflected to obtain two standing waves with orthogonal polarizations, moving in opposite directions. After we mounted the critical retroreflecting mirror on a long, rigid plate to minimize axial vibrations, the average over ten beat notes had a half width at half maximum (HWHM) of 216(10) Hz for a 2-ms pulse [20].

The following procedure is used to acquire a momentum spectrum. At the end of evaporative cooling, the radio frequency knife is held fixed for 6.5 s to allow the cloud to relax to equilibrium. Indeed, we observe axial shape oscillations of the cloud, triggered by the onset of Bose-Einstein condensation [9,21], despite a slow evaporation (less than 100 kHz/s) across T_c. The magnetic trap is then switched off abruptly, in roughly 100 μs, and the cloud expands for 2 ms before the Bragg lasers are pulsed on for 2 ms. We wait for a further 20 ms to let each diffracted component (one per laser standing wave) separate from the parent condensate, and take an absorption image [Fig. 1(a)]. Diffraction efficiency is defined as the fraction of atoms in each secondary cloud. We repeat this complete sequence for several detunings (typically 15), several times (typically 5). After averaging the diffraction efficiencies measured at each detuning δ, we obtain two "elementary spectra," one for each diffraction component.

We take the Bragg spectrum after expansion rather than in the trap to overcome two severe problems. In the trapped condensate, first, the mean-free path (about 10 μm) is much smaller than its axial size, typically 260 μm, so that fast Bragg-diffracted atoms would scatter against the cloud at rest [22]. Second, the inhomogeneous mean-field broadening [2] would be of the order of 300 Hz, i.e., larger than the spectral width expected from phase fluctuations. By contrast, after 2 ms of free expansion, the peak density has dropped by 2 orders of magnitude [23], and both effects become negligible. In addition, the phase fluctuations do not significantly evolve in 2 ms, since the typical time scale for their complete conversion into density ripples varies from 400 ms to 15 s for the range of temperatures we explore [12]. Also, the mean-field energy is released almost entirely in the radial direction, because of the large aspect ratio of the trap [23], and contributes only about 50 Hz of Doppler broadening in the axial direction. The only perturbation of in-trap axial momenta due to the trap release seems to be small overall shifts (around 100 μm/s) attributed to residual magnetic gradients that merely displace the spectra centers.

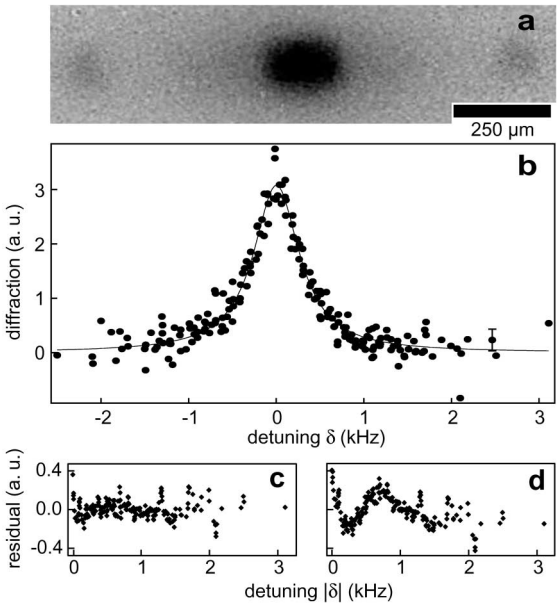

FIG. 1. (a) Absorption image of degenerate cloud (center) and diffracted atoms (left and right), averaged over several shots, after free-flight expansion. (b) Diffraction efficiency versus relative detuning of the Bragg lasers at $T = 261(13)$ nK, with $T/T_\phi = 20(2)$. A typical statistical error bar is shown. This spectrum is the superposition of 12 "elementary spectra" (see text). The true average center is 30.18(2) kHz, close to 30.17 kHz, the four-photon resonance frequency. The solid line is a Lorentzian fit of width 316(10) Hz (HWHM). (c) and (d) show, respectively, the residual of a Lorentzian and of a Gaussian fit to the above spectrum. Residuals are folded around the $\delta = 0$ axis, and smoothed with a six-point-wide sliding average.

Bragg spectra have been taken at various temperatures between 90(10) and 350(20) nK, while T_c varied from 280(15) to 380(20) nK. The temperature was fixed to within 20 nK by controlling the final trap depth to a precision of 2 kHz, and measured from a fit to the wings of an averaged absorption image. The fitting function is an ideal Bose distribution with zero chemical potential, plus an inverted parabolic profile for the quasicondensed cloud. At each temperature, pairs of elementary spectra (described above) were collected across a 125-ms-wide range of hold times to average over residual oscillations and slowly varying fluctuations. All elementary spectra corresponding to the same temperature are reduced to the same surface, background, and center, and superposed, as in Fig. 1(b).

The line shape of the resulting spectra is clearly closer to a Lorentzian than to a Gaussian (see Figs. 1(c) and 1(d)). This is a significant result, because a Lorentzian-like profile is expected for a momentum distribution dominated by phase fluctuations (see [12] and below), in contrast to the Gaussian-like profile expected for a pure condensate [2,11]. From the Lorentzian fit, we extract the measured half-width $\Delta\nu_M$ for each temperature.

The theoretical results obtained in [6,12] do not apply directly to our experiment. In those works, a 3D Thomas-Fermi density profile was assumed, whereas in our case modification of the density profile by the thermal cloud and radial quantum pressure must be accounted for. We find (and discuss below) that a parabolic profile is still a good fit function, but that the usual $T = 0$ relations between μ, L, R, and the number of condensed atoms N_0 are no longer valid. We therefore extend the calculation of the axial correlation function in [12] to an arbitrary density profile, in the local density approximation. In the mean-field regime [4], from the result of [24] for a 1D uniform Bose gas at finite-temperature, we obtain

$$C(s) = \int dz\, n_1(z) \exp\left(-\frac{n_1(0)|s|}{2n_1(z)L_\phi}\right), \tag{1}$$

where $n_1(z) = \int d^2\mathbf{r}_\perp n_0(\mathbf{r}_\perp, z)$ is the axial 1D density of the quasicondensate, while $n_0(\mathbf{r})$ is its 3D density profile. The coherence length near the center of the trap is $2L_\phi$, with $L_\phi = \hbar^2 n_1(0)/(Mk_BT)$. Following Petrov *et al.* [4,6], we define the temperature which delineates the border between coherent and phase-fluctuating condensates as $T_\phi = L_\phi T/L$. Since $n_1(0)$, L, and T are extracted directly from the images, the definitions of L_ϕ and T_ϕ relate the coherence properties to experimentally measured quantities. The axial momentum distribution follows from a Fourier transform of $C(s)$ and is well approximated by a Lorentzian of width $\Delta p_\phi = \alpha\hbar/L_\phi$ (HWHM), with $\alpha = 0.67$ for a parabolic $n_0(\mathbf{r})$ [12]. The predicted spectral half-width is therefore $\alpha\Delta\nu_\phi$, where

$$\Delta\nu_\phi = \frac{2\hbar k_L}{2\pi M L_\phi}. \tag{2}$$

In the following, we will use α as a free parameter to test the theory outlined above.

Figure 2 shows the measured spectral width $\Delta\nu_M$ versus $\Delta\nu_\phi$. The measured widths increase at higher $\Delta\nu_\phi$ as expected. To compare these data to theory, we need to take into account a finite "instrumental" width of the Bragg spectra, including the effect of the mirror vibrations, residual sloshing in the trap, and Fourier broadening due to the 2-ms pulse length (125 Hz HWHM). We assume that all experimental broadenings result in a Gaussian apparatus function of half-width w_G, to be convolved by the Lorentzian momentum profile with a half-width $\alpha\Delta\nu_\phi$. The convolution, a Voigt profile, has a half-width $\alpha\Delta\nu_\phi/2 + \sqrt{w_G^2 + (\alpha\Delta\nu_\phi)^2/4}$. Note that fitting a Voigt profile instead of a Lorentzian to a spectrum gives the same total HWHM to less than 5%, but the Lorentzian shape is too predominant to extract reliably the Gaussian and the Lorentzian contributions to the profile. Using α and w_G as free parameters to fit the data of Fig. 2, we find $w_G = 176(6)$ Hz, and $\alpha = 0.64(5)(5)$. The first uncertainty quoted for α is the standard deviation of the fit value. The second results from calibration uncertainties on the magnification of the imaging system and on the total atom number, which do not affect w_G. The agreement of the measured value of α with the theoretical value 0.67, to within the 15% experimental uncertainty, confirms quantitatively the temperature dependence of the momentum width predicted in Ref. [6]. The coherence length $\hbar/p_\phi$ deduced from this measurement varies between 5.9(8) and 39(4) μm, in the range $6 < T/T_\phi < 28$.

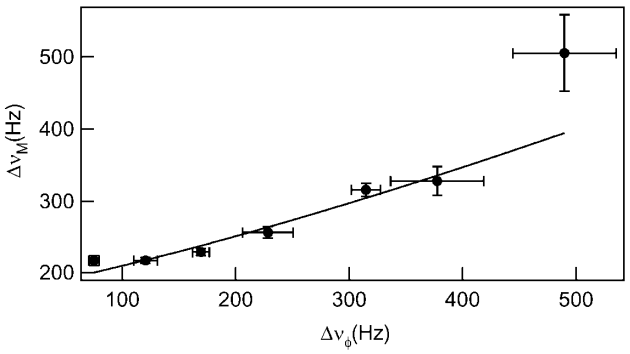

FIG. 2. Half widths at half maximum $\Delta\nu_M$ of the experimental Bragg spectra versus $\Delta\nu_\phi$. Vertical error bars are the standard deviations of the fit width; the horizontal error bars are the one-sigma statistical dispersions of $\Delta\nu_\phi$. The solid line is a fit assuming a Voigt profile for the spectra.

Another important aspect of quasicondensates, the suppression of axial density fluctuations, is investigated here through the size of the trapped condensate. In the presence of density fluctuations, the resulting interaction energy [25] would increase the size with respect to the expectation for a smooth density profile. The measured axial half-length L after release faithfully reflects the half-length in the trap since axial expansion is found experimentally to be negligible. Figure 3 shows that the measured values of L at various temperatures (filled circles) deviate from the standard Thomas-Fermi prediction (diamonds) $L_{TF}^2 = 2\mu/(M\omega_z^2)$, with μ given by $2\mu = \hbar\bar{\omega}(15N_0a/\sigma)^{2/5}$ [16], where $\bar{\omega} = (\omega_\perp^2\omega_z)^{1/3}$, $\sigma = \sqrt{\hbar/(M\bar{\omega})}$, and $a = 5.31$ nm [26]. We understand this smaller value by taking into account the compression of the quasicondensate by the 3D thermal component (excitations with energy much larger than $\hbar\omega_\perp$), and the radial quantum pressure. The 3D excited states contribute negligibly to the fluctuations of the phase [6] and only the density profile is affected. Using a Hartree-Fock approach [16,27], we find

$$L^2 = \frac{2g}{M\omega_z^2}\left\{n_0(0) + \frac{2}{\lambda_T^3}[g_{3/2}(e^{-gn_0(0)/(k_BT)}) - g_{3/2}(1)]\right\}, \tag{3}$$

with the coupling constant $g = 4\pi\hbar^2 a/M$, the thermal de Broglie wavelength $\lambda_T = [2\pi\hbar^2/(Mk_BT)]^{1/2}$, and $g_{3/2}(x) = \sum_{n=1}^{\infty} x^n/n^{3/2}$. The open circles in Fig. 3 show the solution of Eq. (3) assuming a parabolic profile, such

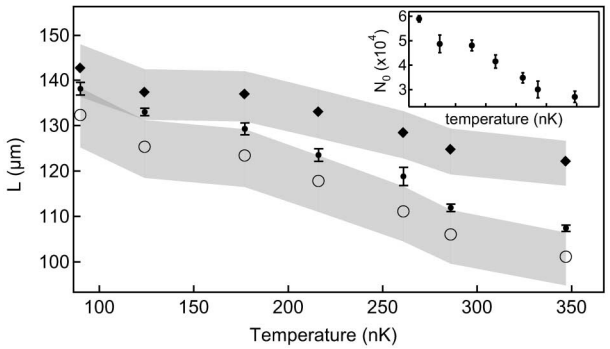

FIG. 3. Half-length L of the quasicondensate versus temperature. Experimental values (● with statistical error bars) are compared to two calculations: standard Thomas-Fermi (◆) and Hartree-Fock with radial quantum pressure corrections (see text) (○). Calculations use the measured temperature and number of condensed atoms. The greyed areas represent uncertainty associated with atom number calibration. Inset: Number of condensed atoms N_0 with statistical dispersion at each temperature.

that $n_0(0) = 15N_0L^{-3}\epsilon^2/(8\pi)$. The aspect ratio ϵ is calculated according to the theory developed in [29], which takes into account radial quantum pressure. The calculated lengths are in agreement with our measurements to within our estimated calibration uncertainty. We conclude, in line with [8], that a phase-fluctuating condensate has the same smooth profile as a true condensate [29], and thus that the axial density fluctuations are suppressed even when phase fluctuations are large.

In conclusion, we have demonstrated three important features of quasi–Bose-Einstein condensates: (i) the momentum distribution shape, found Lorentzian; (ii) the temperature dependence of the momentum width; and (iii) the suppression of density fluctuations. Our results are in quantitative agreement with the finite-temperature, interactive theory developed in [4,6] supplemented by a Hartree-Fock treatment of 3D excited states. The same method could be applied to investigate how long range order develops during the condensate growth.

We thank M. Lécrivain and V. Boyer for the development of the electromagnet trap used in this work, and J. Retter for useful comments on the manuscript. We also thank G.V. Shlyapnikov and D. S. Petrov for stimulating interactions, and S. Gupta and N. Davidson for useful conversations. M. H. acknowledges support from IXSEA. This work was supported by CNRS, DGA, and EU.

Note added.—We would like to point out that complementary work [30] using interferometry was reported soon after the submission of this manuscript.

*Current address: Department of Physics, University of Toronto, Canada.

[1] E.W. Hagley *et al.*, Phys. Rev. Lett. **83**, 3112 (1999).
[2] J. Stenger *et al.*, Phys. Rev. Lett. **82**, 4569 (1999).
[3] I. Bloch, T.W. Hänsch, and T. Esslinger, Nature (London) **403**, 166 (2000).
[4] D. S. Petrov, G.V. Shlyapnikov, and J.T.M. Walraven, Phys. Rev. Lett. **85**, 3745 (2000).
[5] J. O. Andersen, U. Al Khawaja, and H.T.C. Stoof, Phys. Rev. Lett. **88**, 070407 (2002); D. L. Luxat and A. Griffin, Phys. Rev. A **67**, 043603 (2003); C. Mora and Y. Castin, Phys. Rev. A **67**, 053615 (2003).
[6] D. S. Petrov, G.V. Shlyapnikov, and J.T.M. Walraven, Phys. Rev. Lett. **87**, 050404 (2001).
[7] S. Dettmer *et al.*, Phys. Rev. Lett. **87**, 160406 (2001); D. Hellweg *et al.*, Appl. Phys. B **73**, 781 (2001).
[8] H. Kreutzmann *et al.*, Appl. Phys. B **76**, 165 (2003).
[9] I. Shvarchuck *et al.*, Phys. Rev. Lett. **89**, 270404 (2002).
[10] J. Steinhauer *et al.*, Phys. Rev. Lett. **88**, 120407 (2002).
[11] F. Zambelli *et al.*, Phys. Rev. A **61**, 063608 (2000).
[12] F. Gerbier *et al.*, Phys. Rev. A **67**, 051602(R) (2003).
[13] Note that this definition of the coherence length is different from L_ϕ (see later in the text).
[14] B. Desruelle *et al.*, Phys. Rev. A **60**, R1759 (1999).
[15] The atom number measurement is calibrated to a 20% precision by comparing a measurement of N_c to theory [16].
[16] F. Dalfovo *et al.*, Rev. Mod. Phys. **71**, 463 (1999).
[17] F. Schreck *et al.*, Phys. Rev. Lett. **87**, 080403 (2001); A. Görlitz *et al.*, Phys. Rev. Lett. **87**, 130402 (2001); M. Greiner *et al.*, Phys. Rev. Lett. **87**, 160405 (2001); see also E. H. Lieb, R. Seiringer, and J. Yngvason, cond-mat/0304071, and references therein.
[18] S. Stringari, Phys. Rev. A **58**, 2385 (1998).
[19] P. B. Blakie, R. J. Ballagh, and C.W. Gardiner, Phys. Rev. A **65**, 033602 (2002); M. D. Girardeau and E. M. Wright, Phys. Rev. Lett. **87**, 050403 (2001).
[20] Since supplementary mirrors must be added to perform this measurement, the result is an upper limit to the linewidth of δ.
[21] F. Gerbier *et al.*, cond-mat/0210206.
[22] A. P. Chikkatur *et al.*, Phys. Rev. Lett. **85**, 483 (2000).
[23] Y. Castin and R. Dum, Phys. Rev. Lett. **77**, 5315 (1996); Yu. Kagan, E. L. Surkov, and G.V. Shlyapnikov, Phys. Rev. A **55**, R18 (1997).
[24] J.W. Kane and L. P. Kadanoff, Phys. Rev. **155**, 80 (1967).
[25] W. Ketterle and H.-J. Miesner, Phys. Rev. A **56**, 3291 (1997).
[26] E. G. M. van Kempen *et al.*, Phys. Rev. Lett. **88**, 093201 (2002).
[27] V.V. Goldman, I. F. Silvera, and A. J. Leggett, Phys. Rev. B **24**, 2870 (1981); S. Giorgini, L. P. Pitaevskii, and S. Stringari, J. Low Temp. Phys. **109**, 309 (1997).
[28] A. L. Zubarev and Y. E. Kim, Phys. Rev. A **65**, 035601 (2002).
[29] For a 1D gas, relative density fluctuations $\langle[\delta n/n_0(0)]^2\rangle$ are predicted not to exceed a few percent [4] with our experimental parameters. Systematic uncertainties, however, prevent us from observing them.
[30] D. Hellweg *et al.*, Phys. Rev. Lett. 91, 010406 (2003).